UNIVERSITY OF BIRMINGHAM

Characterising premixed ammonia and hydrogen combustion for a novel Linear Joule Engine Generator

Zhang, Fangyu; Chen, Gen; Wu, Dawei; Li, Tie; Zhang, Zhifei; Wang, Ning

Link to publication on Research at Birmingham portal

Characterising Premixed Ammonia and Hydrogen Combustion for a Novel Linear Joule Engine Generator

*Fangyu Zhang [1], Gen Chen [1], Dawei Wu [1, *], Tie Li [2], Zhifei Zhang [2] and Ning Wang [2]*

[1] School of Engineering, University of Birmingham, Birmingham, United Kingdom, B15 2TT

[2] School of Naval Architecture, Ocean & Civil Engineering, Shanghai Jiao Tong University, Shanghai, China, 200240

Abstract: A novel ammonia/hydrogen dual-fuelled Linear Joule Engine Generator (LJEG) is developed for medium to large scale power generations and electrification of ship propulsion systems. The characteristics of premixed ammonia/hydrogen combustion of the LJEG are investigated through chemical kinetic modelling. Three representative mechanisms are compared based on their accuracy of reproducing experimental results. With robust combustion and low NO_x emission as the primary targets, laminar burning velocity, ignition delay and flame species concentration are investigated over a wide range of equivalence ratio $(0.8 - 1.6)$, hydrogen blending ratio $(0.0 - 0.6)$, oxygen content $(0.21 - 1.00)$, inlet temperature $(300\ K - 700\ K)$ and pressure $(1\ bar - 20\ bar)$. Rate of production (ROP) analysis is carried out to gain in-depth understanding of critical NO production and consumption pathways. The results indicate that an equivalence ratio around 1.1 is beneficial for both combustion robustness and NO_x emission reduction. Both adding hydrogen in the fuel $(40\% Vol)$ and enriching oxygen in the oxidizer $(60\% Vol)$ promote burning velocity to the similar level of methane $(37\ cm/s)$. Explicit reduction of NO emission is observed when pressure increases, which can be attributed to the combination of NH_i radicals. The findings show the potential of the ammonia and hydrogen fuelled LJEG for ultra-low emission power generation.

Keywords: Ammonia-hydrogen premixed combustion, Linear Joule Engine Generator, Chemical kinetics model, Oxygen enrichment

Nomenclature	
ϕ	Fuel-air equivalence ratio
$x\% H_2$	Hydrogen blending ratio (hydrogen mole fraction in fuel)
$E\% NH_3$	Ammonia fraction by energy
Ω	Oxygen content (oxygen mole fraction in oxidizer)
T	Inlet temperature (K)
P	Inlet pressure (bar)
S_L	Laminar burning velocity (cm/s)
τ	Ignition delay time (ms)
$x[i]$	Mole fraction of i
$x[i]'_{end}$	Normalized outlet mole fraction of i
$x[i]_{end}$	Outlet mole fraction of i
$x[i]_{start}$	Inlet mole fraction of i

1. Introduction

Ammonia is regarded as a good hydrogen carrier, while it could be considered as an alternative zero-carbon fuel

---

* Corresponding author.

E-mail address: d.wu.1@bham.ac.uk (D.Wu).

29   [1, 2]. With no carbon in the molecule of ammonia, no carbon-related gaseous and soot emissions will be emitted
30   from ammonia combustion. The recent progress in power-to-gas technologies and other renewable derived
31   methods enables ammonia production using renewable energy, which almost eliminates any carbon footprints in
32   the lifecycle of using ammonia as a fuel [3, 4]. Availability of combustion engines to adapt to ammonia as a fuel
33   is crucial for wide applications. Due to lack of diesel during the World War II, ammonia was temporarily used as
34   a fuel in internal combustion engines for buses in Belgium [5]. In the 1960s, the feasibility and performance of
35   using ammonia for reciprocating engines and gas turbines were studied by the U.S. Army [6, 7]. In 2017, National
36   Institute of Advanced Industrial Science and Technology (AIST) in Japan implemented a $50\ kW$ micro gas
37   turbine power generations using pure ammonia diffusion combustion [8]. The project aligned with a Japanese
38   national technology development project, "Cross-ministerial Strategic Innovation Promotion Program (SIP):
39   Energy carrier" launched to promote hydrogen utilization in 2014 [9]. Apart from conventional heat engines,
40   new power generation technologies have been considered to take ammonia and hydrogen. Free piston engine
41   applying external combustion integrates with a linear alternator to form a novel Linear Joule Engine Generator
42   (LJEG), which was proposed in 2014 [10]. Recently, a further development of LJEG using hydrogen fuel has
43   been published to demonstrate the potential [11]. LJEG hires Joule Cycle/Brayton Cycle same as gas turbines
44   while has a high thermal efficiency of $33-45\%$ even in small kW scales [11] compared to a typical $30-$
45   40% of gas turbines in the range of $5-50\ $ MW [12]. In contrast to internal combustion engines, heat addition
46   process of LJEG takes place outside of cylinders, which allows continuous combustion if coupling with multiple
47   expansion cylinders. This may potentially make it much easier to apply some measures to avoid ammonia slip
48   and reduce NO_x emission. LJEG is dedicated to electricity generation which requests it working mostly in
49   constant frequencies and rated loads. This would benefit for LJEG to achieve stable combustion conditions,
50   thereby better thermal efficiency. The development of the LJEG prototypes, including both mechanical and
51   electrical designs, can be viewed in the published papers [13, 14], however a detailed design of an external
52   combustion reactor would be essential to achieve the full potential of an ammonia fuelled LJEG. With ammonia
53   as the main fuel, two major obstacles of ammonia combustion must be overcome: slow combustion and high
54   NO_x emission. An in-deep understanding on the fundamental characteristics of premixed combustion of
55   ammonia under the working conditions of LJEG is critical to deal with those challenges and successfully develop
56   an ammonia fuelled LJEG.
57
58   ## 2. The state of the art in characterising ammonia combustion
59   Ammonia is well-known for its narrow flammability (around $18\%-28\%$ fuel mole fraction) [2], high ignition
60   temperature and low burning velocity. It is reported that using ammonia alone for spark ignition internal
61   combustion engine is hard to achieve satisfactory performance [15]. To stabilize ammonia combustion, it is
62   necessary to add promoters such as hydrocarbon fuel [16-18] or hydrogen [19-21]. Hydrogen is also a carbon-
63   free fuel which could be obtained from ammonia thermal cracking or from a separate fuel line. It is more
64   attractive than hydrocarbons to be used as a promoter in ammonia combustion. The stability limits of premixed
65   ammonia/hydrogen and ammonia/methane flame were tested with a generic swirl combustor under $1-5\ bar$
66   [22]. The result shows an interesting feature of ammonia/hydrogen blends that $40\%NH_3/60\%H_2$ flame can be
67   stable even under very fuel-lean conditions $(\phi{\sim}0.3)$ while the minimum stable equivalence ratio for
68    $40\%NH_3/60\%CH_4$ flame is 0.6. Lee *et al.* experimentally and computationally investigated premixed
69   ammonia/hydrogen flames under ambient temperature and pressure conditions for hydrogen production [19]. It
70   was observed that the laminar burning velocity is substantially improved with the hydrogen mole fraction rising
71   in the fuel from 0.0 to 0.5, under fuel-rich conditions.
72

There have been a handful studies on ignition delay in premixed pure ammonia or ammonia blended with methane combustion, but few studies on ignition delay in premixed ammonia and hydrogen combustion so far. Ignition delay time of ammonia in highly diluted Ar $(98-99\%)$ was measured by Mathieu *et al.* to investigate the effects of temperature $(1560-2455\ K)$, pressure $(1.4, 11, 30\ atm)$ and equivalence ratio $(0.5, 1.0, 2.0)$ [23]. The experiment outcomes were validated with several ammonia mechanisms, finding many mechanisms are hard to predict the ignition delay accurately. Xiao *et al.* [17] improved the ignition chemistry for a detailed ammonia chemical kinetic reaction mechanism which is mostly based on Konnov's mechanism [24]. Ignition delay is predicted with several specific equivalence ratios $(0.6, 1.0, 1.4)$ and various ammonia concentrations $(0\%-100\%)$ at $2000\ K$. It showed that ignition delay increases monotonically with ammonia concentration and equivalence ratio.

Other methods to stabilize ammonia combustion include increasing oxygen content in the oxidizer [25-27] or using strong oxidants [28]. The oxy-fuel combustion is a process whereby combustion is kept in a nearly pure oxygen environment. This is a commonly used method in hydrocarbon combustion in order to maintain flame robustness [29, 30]. Mei *et al.* [27] studied experimentally and numerically the effect of oxygen content in the oxidizer in the range of $25\%-45\%$ on premixed laminar flame speed of ammonia. The oxygen enrichment effectively enhances ammonia flames and minimizes the buoyancy effect. The effect of oxygen content varying from 21% to 30% on ammonia oxidation was studied numerically under atmospheric pressure [25]. The results show that laminar burning velocity with 30% oxygen in the oxidizer is around 2.6 times of that with 21% oxygen in the oxidizer. The increase of oxygen content in the oxidizer promotes HNO formation, as a result, NO formation increases at the post-flame zone.

NO_x emission is another important issue to be discussed when pure ammonia or ammonia/hydrogen combustion is applied in heat engines. NO_x emission is affected when hydrogen is blended into ammonia. Ammonia has a lower heating value than that of hydrogen, resulting in lower temperature in ammonia/hydrogen combustion. Therefore, thermal-NO_x from ammonia/hydrogen combustion is lower than that from pure hydrogen combustion. Meanwhile, fuel-bound NO_x is dominate in ammonia/hydrogen combustion. It is important to discuss the role of NO_x formation pathways under different working conditions to minimize NO_x emission. Burner experiments with $50\%vol\ NH_3/50\%vol\ H_2$ blend in a swirl combustor were conducted at Cardiff University [20]. The flame is stable at an equivalence ratio of $0.43-0.52$. It was found that excessive OH and O radicals result in a higher NO_x emission (in the range of thousands of ppm) compared to fuel-rich conditions. Li et al. [31] numerically investigated the NO_x emission of a staged NH_3/H_2 combustor which consists of a rich-burn stage and a lean-burn stage. The equivalence ratio of the rich-burn stage is observed to be critical and more sensitive than the equivalence ratio of the whole system in minimizing NO_x emission. This may assist to broaden the range of secondary air inlet amount without NO_x penalties.

Although ammonia combustion experiments have provided some important outcomes, further investigations with numerical studies are required to extend understandings of ammonia combustion in different working conditions which is constrained due to limited experimental rigs and available measurement methods. An appropriate ammonia chemical kinetic mechanism is the basis for simulating ammonia combustion. Fundamental combustion research of ammonia chemical kinetic mechanisms is extensively reviewed. The nitrogen chemistry relevant to NO_x formation (including Zel'dovich mechanism, prompt NO_x and fuel-bound NO_x) was proposed and compared with the experimental data by Miller and Bowman in 1989 [32]. Konnov [24] developed a detailed chemical mechanism containing 127 species and over 1200 reactions which can be used for ammonia blends

117 with hydrogen and small hydrocarbons. A comprehensive mechanism for $NH_3/H_2/CH_4$ including 128
118 species and 957 reactions were developed by Li et al. [33]. The mechanism was then reduced using directed
119 relation graph with error propagation (DRGEP) and DRGEP with sensitivity analysis (DRGEPSA) method for
120 CFD modelling implement. Duynslaegher *et al.* [34, 35] conducted experiments with premixed $0.21NH_3/$
121 $0.13H_2/0.21O_2/0.45Ar$ (mole fraction) flames under low pressure conditions (0.05 – 0.12 *bar*) and
122 systematically examined five mechanisms (i.e. GRI [36], San Diego [37], Lindstedt *et al.* [38], Bian [39] and
123 Konnov [24, 40]) for their prediction accuracies. Konnov's mechanism aligns with the experiment outcomes
124 very well, although discrepancies were found in the concentrations of N_2O and NH_2. Duynslaegher *et al.*
125 improved the prediction accuracy of N_2O and NH_2 and further reduced the mechanism to 19 species and 80
126 reactions [34]. Song *et al.* [41] developed the mechanism according to the experiment of ammonia oxidation at
127 high temperature (450-925 *K*) and high pressure (30 and 100 bar). The reactions at high pressure are
128 emphasized in the mechanism. Following Song's work, Otomo *et al.* [42] revised the reactions related to NH_2,
129 HNO and N_2H_2 and the refined mechanism is also utilized to predict ammonia/hydrogen combustion in terms
130 of flame speed, ignition delay and unburnt ammonia and NO_x emission. More recently, Nakamura et al. [43]
131 developed an ammonia chemical kinetic mechanism which is based on Miller and Bowman's mechanism [32].
132 The $H_2/NH_x/N_2O/NNH$ chemistry is improved from the study of Mathieu and Petersen [23]. The chemistry
133 of N_2H_x except NNH is adopted from the study of Konnov [24]. Additionally, the thermochemical properties
134 calculated by Bugler et al. [44] is also applied in the improved mechanism. The species concentrations generated
135 from the improved mechanism aligned with the measurements. The flame speed and ignition delay results were
136 verified with literature data. In order to investigate the autoignition behaviour of ammonia and
137 ammonia/hydrogen mixtures, Dai et al. presented a mechanism validated with the experimental data under $20 -$
138 75 *bar* at $1040 - 1210$ *K* [45]. It shows the mechanism has a good agreement with the measured ignition
139 delay time of NH_3 and NH_3/H_2 under $40 - 60$ *bar*.

141 Most of the previous studies on chemical kinetic mechanisms focuses on fundamental combustion chemistries
142 of pure ammonia or ammonia/hydrocarbon (methane, in particular). Few works reported the characteristics of
143 premixing ammonia/hydrogen combustion for applications with similar working conditions in the proposed
144 LJEG. Even less works can be found on the effect of oxygen enrichment on ammonia or ammonia/hydrogen
145 premixing combustion. To develop an optimal external combustor of the LJEG prototype, it is essential to identify
146 a suitable chemical kinetic mechanism to extend the understanding of ammonia/hydrogen premixing combustion
147 under the typical LJEG working conditions. In the paper, characteristics of premixed ammonia/hydrogen
148 combustion are studied under typical LJEG operational conditions. Two relatively new mechanisms developed
149 by Otomo *et al.* [42] and Nakamura *et al.* [43], and another Duynslaegher's mechanism [34] with improved NO
150 prediction, are selected as representative ammonia combustion mechanisms to be compared with the published
151 experimental results from the comprehensive literature review. Laminar burning velocity, ignition delay and
152 species concentrations are investigated over a wide range of equivalence ratios, hydrogen blending ratios, oxygen
153 content in the oxidizer, inlet temperature and pressure. The best ammonia combustion mechanism will be
154 identified for a further parametric study. The findings of this study will provide a clear guidance on determining
155 operational parameters and optimal design of the external combustion reactor in the LJEG, and even more
156 potential applications like ammonia fuelled gas turbines, etc.

158 **3. Methodology**
159 The schematic diagram of the proposed ammonia/hydrogen duel fuelled LJEG is shown in Figure 1. The LJEG
160 mainly consists of the following components: a linear compressor, a linear expander, an external reactor, and a

161 linear alternator. Two double-acting pistons are applied in the compressor and the expander, respectively, which
162 separate cylinders into two opposite chambers. Compared to conventional single acting design, the double acting
163 design is expected to enhance output power while alleviating harshness caused by pulsating gas exchange flow.
164 The two pistons are connected by a rigid driving shaft, where moving magnets are installed and act as the
165 translator of the linear alternator. On the expander cylinder heads, camless poppet valves are used to control the
166 intake and exhaust gas flows in terms of real-time piston displacement, in-cylinder pressure and temperature.
167 Reed valves are used to regulating gas exchange process of the compressor.

169 Heat is introduced into the LJEG through ammonia and hydrogen combustion in the external reactor. The ideal
170 thermodynamic cycle applied in the LJEG consists of four processes. An adiabatic compression process happens
171 in the compressor of LJEG. The external combustor operates at a constant pressure, where heat addition takes
172 place through premixed ammonia and hydrogen combustion. When hot exhaust gas from the combustor enters
173 the expander, the piston is driven by gas expansion to do linear motion. The mechanical power deducing friction
174 losses is used to drive the compressor piston for the compression process, and the translator of the alternator for
175 power generation. After the expansion process, used gas is rejected into the environment as a constant pressure
176 heat rejection process. The working conditions of the LJEG are identified, therefore, the ranges of interested
177 input parameters are determined for the combustion model mentioned below.
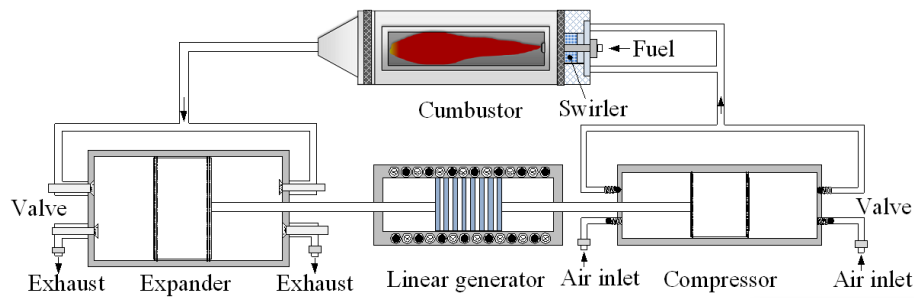
179 Figure 1. Schematic diagram of the LJEG

180 For any ammonia combustion devices, ammonia slip is a foremost issue to be dealt with. The burning velocity
181 of ammonia is much lower than conventional hydrocarbon fuels, therefore it is essential to understand the
182 influence of various parameters on ammonia burning velocity and find a way to accelerate ammonia combustion.
183 In this study, 1D premixed freely propagating flame sub-model in ANSYS CHEMKIN PRO is used to calculate
184 premixed laminar burning velocity over a wide range of equivalence ratio $(0.8 - 1.6)$, hydrogen blending ratio
185 $(0.0 - 0.6)$, oxygen content in the oxidizer $(0.21 - 1.00)$, inlet temperature $(300 - 700\ K)$ and pressure
186 $(1 - 20\ bar)$. The hydrogen blending ratio, $x\%H_2$, and the oxygen content, Ω, are defined as the mole fraction
187 of hydrogen in the fuel mixture and mole fraction of oxygen in the oxidizer, respectively. They are determined
188 by:

$$x\%H_2 = \frac{x[H_2]}{x[H_2]+x[NH_3]}\ , \tag{1}$$

$$\Omega = \frac{x[O_2]}{x[O_2]+x[N_2]}\ , \tag{2}$$

189 where $x[H_2]$, $x[NH_3]$, $x[O_2]$ and $x[N_2]$ denote the mole fraction of hydrogen, ammonia, oxygen and
190 nitrogen, respectively. Another important property for premixed ammonia/hydrogen combustion is ignition delay
191 which is usually measured with shock tube in experiments. It is defined as the time interval between the start of
192 injection and the start of combustion. Due to the limited range of flammability and high ignition temperature of
193 ammonia combustion, understanding the influence of various parameters on ignition delay can provide the

guidance to improve the ignition of ammonia. In this work, the 0D closed homogeneous reactor sub-model in ANSYS CHEMKIN PRO is utilized to predict the ignition delay time. It is calculated at isobaric and adiabatic conditions and can be determined as the time during which a certain species concentration reaches its maximum or the inflection point of temperature appears. In this study, ignition delay is defined as the time to reach the maximum concentration of OH. Various parameters such as equivalence ratio $(0.5, 1.0, 1.5)$, hydrogen blending ratio $(0.0 - 1.0)$, oxygen content $(0.21 - 1.00)$, inlet temperature $(1400 - 2200 \; K)$ and inlet pressure $(1 - 20 \; bar)$ is analysed.

One of the key targets for developing ammonia-fuelled LJEG is to minimize NO_x emission, as fuel-bound NO_x is expected to play an important role in addition to the thermal NO_x. Thus, the knowledge of ammonia flame structure and the production and consumption process of nitric oxide is critical. In this study, flame structure is investigated with a burner-stabilized flame sub-model in ANSYS CHEMKIN PRO. The species mole fraction profiles of fuels (NH_3 and H_2) and NO_x (NO, N_2O and NO_2) are analysed under a wide range of equivalence ratios $(0.9 - 1.2)$, hydrogen blending ratios $(0.0 - 0.8)$, oxygen contents $(0.21 - 1.00)$ and inlet pressure $(1 - 20 \; bar)$. Besides, considering that the inlet ammonia concentration varies with other inlet conditions, NO_x emission concentrations are also normalized against the inlet ammonia concentrations to avoid the influence on results interpretation, i.e.:

$$x[NO_x]'_{end} = \frac{x[NO_x\;]_{end}}{x[NH_3]_{start}}, \qquad (3)$$

where $x[NO_x]'_{end}$, $x[NO_x\;]_{end}$ and $x[NH_3]_{start}$ denote mole fraction of normalized NO_x emission, NO_x emission and inlet NH_3, respectively. NO_x refers to NO, NO_2, N_2O. The characteristics of premixed ammonia/hydrogen combustion and the kinetic models used provide a solid basis of studying turbulent flame in the external reactor for an optimal design.

4. Mechanism validation

In order to select the most suitable mechanism for further parametric study, the comparison between three selected representative mechanisms against the same sets of experimental data is carried out. The details of the three representative mechanisms are shown in Table 1.

Table 1 Summary of the selected mechanisms

Mechanisms	Number of species	Number of elementary reactions	Mixture	Parameters validated in previous work
Duynslaegher's mechanism [34]	19	80	$NH_3/H_2/O_2/Ar$	Species profiles, laminar flame speed [46]
Otomo's mechanism [42]	32	213	NH_3/air, NH_3/H_2/air	Ignition delay, species profiles, laminar flame speed
Nakamura's mechanism [43]	33	232	NH_3/air	Species profiles, ignition delay, laminar flame speed

222 For burning velocity validation, the measured data of premixed ammonia/hydrogen blends under standard
223 temperature and pressure (STP) performed by Kumar et al. [47] is used. Figure 2 demonstrates the burning
224 velocity of ammonia/hydrogen as a function of equivalence ratio at various ammonia fraction by energy. The
225 numerical results show that Duynslaegher's reduced mechanism [34] agrees better with the measured data when
226 hydrogen is the primary fuel in the blends ($E\%NH_3 = 20\%$). Otomo's mechanism [42] and Nakamura's
227 mechanism [43] have better predictions when ammonia is the primary fuel in the blends ($E\%NH_3 = 50\%$ and
228 $E\%NH_3 = 80\%$). Since ammonia is the primary fuel for the proposed LJEG, Otomo's mechanism and
229 Nakamura's mechanism are considered more suitable for predicting ammonia burning velocity.
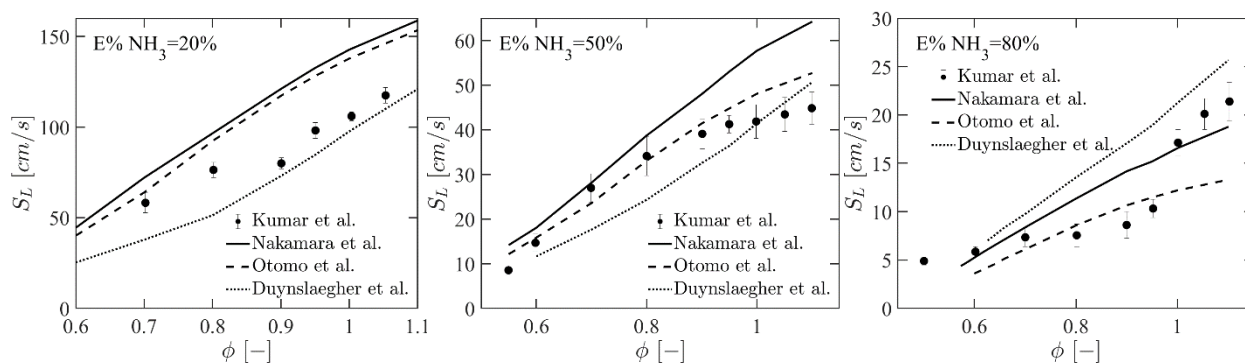
230

231 Figure 2. Comparison between experimental and computational premixed NH_3/H_2 laminar burning velocity
232 when $E\%NH_3$ is (a) 20%, (b) 50% and (c) 80%. Experimental results by Kumar et al. [47] plotted in
233 conjunction with computational results using Nakamura's mechanism [43], Otomo's mechanism [42] and
234 Duynslaegher's reduced mechanism [34].

235 Mathieu et al. [23] conducted the shock tube experiments to measure the ignition delay time of $NH_3/O_2/Ar$
236 blends at $1.4, 11, 30\ atm$. The ignition delay time was defined as the time between the passage of the reflected
237 shock wave and the intersection of the slope of hydroxyl radical (OH^*) and the zero-concentration horizontal
238 line. As shown in Figure 3, modelling with Nakamura's mechanism agrees well with the experimental data, while
239 predictions based on Otomo's mechanism [42] are slightly overestimated and a significant discrepancies among
240 the predictions and measurements are found using Duynslaegher's reduced mechanism [34], which is mainly
241 because the initial mechanism was only validated with low pressure experimental results.
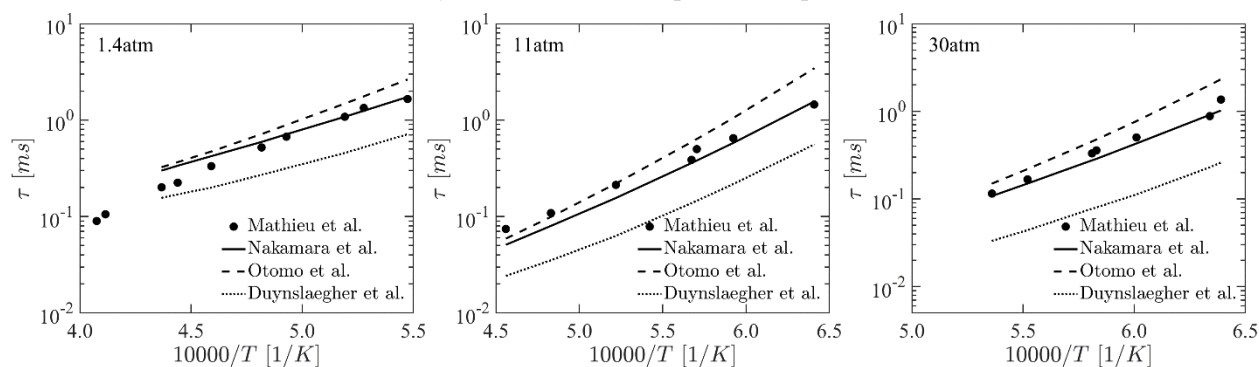
242

243 Figure 3. Comparison between experimental and computational ignition delay time for the case of
244 $0.01143NH_3/0.00857O_2/0.98Ar$ $(\phi = 1.0)$ at (a) $1.4\ atm$, (b) $11\ atm$ and (c) $30\ atm$. Experimental
245 results by Mathieu et al. [23] plotted in conjunction with computational results using Nakamura's mechanism,
246 Otomo's mechanism and Duynslaegher's reduced mechanism.

247 The species profiles of premixed $0.21NH_3/0.13H_2/0.21O_2/0.45Ar$ flame at a low pressure $(0.05\ bar)$ was
248 measured by Duynslaegher [35]. It is shown in Figure 4 that the modelling results for profiles of NH_3, H_2 and

7

249   N_2 with all three mechanisms all have satisfactory agreement with the measured results. The best agreement
250   with the measured profiles of NO, N_2O and NH_2 is achieved by using Duynslaegher's reduced mechanism,
251   though the peak mole fractions of NO and N_2O are still underestimated.
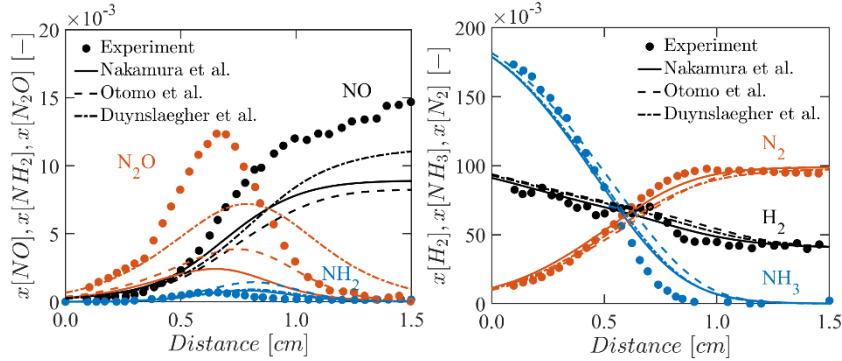
253 Figure 4. Comparison between experimental and computational concentration profiles of (a)NO, NH_2, N_2O and
254 (b)NH_3, H_2, N_2 for the case of $0.21NH_3/0.13H_2/0.21O_2/0.45Ar$ at $0.05\ bar$. Experimental results by
255 Duynslaegher *et al.* [35] plotted in conjunction with computational results using Nakamura's mechanism,
256 Otomo's mechanism and Duynslaegher's reduced mechanism.

257 <div align="center">Table 2 The comparison of three selected mechanisms</div>

Mechanisms	Burning velocity	Ignition delay	Main species profiles
Duynslaegher's mechanism	↑*	↓	↑↑
Otomo's mechanism	↑	↑	↓
Nakamura's mechanism	↑	↑↑	↑

258 *The symbols ↑↑,↑,↓ indicate 'good agreement', 'acceptable discrepancy', and 'significant discrepancy', respectively.

259   To compare the overall performance of three mechanism candidates, Table 2 demonstrates their performance in
260   terms of three individual parameters of the greatest interest. Modelling results with Nakamura's and Otomo's
261   mechanism could predict better in premixed NH_3/H_2 laminar burning velocity and ignition delay. In regard to
262   flame species concentrations, Duynslaegher's reduced mechanism has better agreement than the other two
263   mechanisms, although a significant difference is found between the measured and computational ignition delay
264   time. Between Otomo's and Nakamura's mechanisms, the latter predicts much better in NO profile. Therefore,
265   Nakamura's detailed reaction kinetic mechanism is selected for the further parametric analysis of premixed
266   NH_3/H_2 combustion under the prevalent working conditions of the LJEG.

267

268 **5. Results and discussion**
269 **5.1 Premixed laminar burning velocity**
270   Premixed laminar burning velocity is defined as the velocity at which the flame front propagates towards the
271   unburned mixture, which is one of the most important combustion properties to provide the evidence of ammonia
272   flame robustness in the LJEG. Premixed laminar burning velocity of $NH_3/H_2/Air$ mixture is investigated under
273   various equivalence ratio and hydrogen fractions at the inlet temperature of $300\ K$ and inlet pressure of $1\ bar$
274   in Figure 5(a). It shows that increasing hydrogen fractions significantly enhance the burning velocity, which
275   attributes to the high reactivity of hydrogen with a laminar burning velocity over $250\ cm/s$ at NTP (normal
276   temperature and pressure) compared to only $7\ cm/s$ of ammonia flames [48-50]. The high reactivity of
277   hydrogen may cause flame to burn backwards, leading to flashback in boundary layer [20], which should be
278   avoid and treated with cautions in the external combustor of LJEG. It is worth noting that laminar burning
279   velocity peaks when equivalence ratio is around $1.1-1.2$ in all cases of different hydrogen fractions. It can be

concluded that an equivalence ratio within the range of $1.1 - 1.2$ is favourable to improve the stability of ammonia premixed combustion with hydrogen in presence working as a combustion promoter. The laminar burning velocity of $60\%NH_3/40\%H_2$ fuel blend reaches $34\ cm/s$ at the equivalence ratio of 1.1, which is equivalent to that of methane flames $(\sim37\ cm/s)$ under similar conditions [16].

To investigate optimal combustion conditions in the ammonia fuelled LJEG, the premixed laminar burning velocity of a pure ammonia flame and a flame of $70\%NH_3/30\%H_2$ blend is plotted as a function of inlet temperature and inlet pressure in Figure 5(b) ($\phi = 1.1$). Inlet temperature has a positive effect on the burning velocity of both the ammonia flame and the ammonia/hydrogen flame, therefore increased temperature at the compressor outlet of the LJEG may increase burning velocity, especially when hydrogen promoter is in presence. At atmospheric pressure, the burning velocity of the ammonia/hydrogen flame increases by around $90\ cm/s$ compared to an increase of around $40\ cm/s$ of the pure ammonia flame, when the inlet temperature increases from $300\ K$ to $700\ K$. Conversely, increasing inlet pressure results in a decrease of burning velocity. For example, the burning velocity of ammonia/hydrogen decreases by approximately $30\ cm/s$ at $700\ K$, when the inlet pressure rises from $1\ bar$ to $5\ bar$. It is also observed that the adverse impact of high inlet pressure on burning velocity is weakened if inlet pressure further increases from $5\ bar$ to $20\ bar$. In a typical LJEG work condition (inlet pressure of $15\ bar$ and inlet temperature of $600\ K$), the burning velocity of the $70\%NH_3/30\%H_2$ flame has the potential to reach $40\ cm/s$. While an even higher pressure may improve the LJEG efficiency, it may cause a small penalty on the burning velocity of ammonia/hydrogen flame.

Potential of hydrogen-oxy combustion used in the closed-cycle LJEG has been discussed in a recent paper [11], which demonstrates a clean power generation solution with water as the only emission. Although ammonia-oxy combustion cannot eliminate NO_x due to inevitable fuel-bound NO formation, oxygen enrichment brings substantial benefit to burning velocity of ammonia flame. Figure 5(c) illustrates the premixed laminar burning velocity increases with an increasing oxygen fraction in oxidizer at equivalence ratio of 1.1 under NTP. Oxygen enrichment increases adiabatic temperature, thereby increasing the laminar combustion speed. The same trend was recorded in hydrocarbon combustion [51, 52]. With 60% oxygen content in the oxidizer, pure ammonia flame achieves a similar flame speed as that of methane flame under NTP ($37\ cm/s$) [16]. When 30% hydrogen and 70% ammonia fuel mixture is used, 30% oxygen content in the oxidizer assists the burning velocity to reach $39\ cm/s$, equivalent to that of methane again.
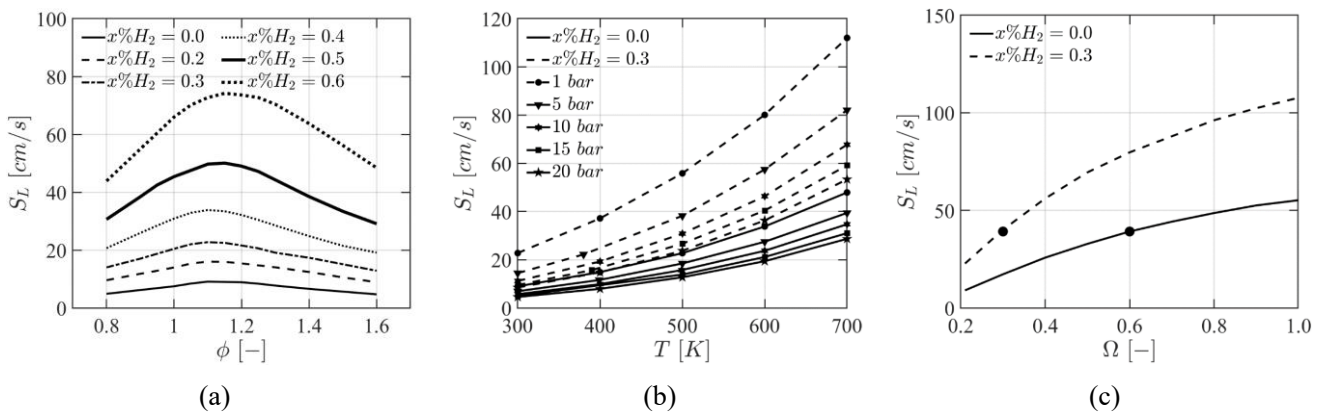

(a) (b) (c)

Figure 5. Variation of premixed laminar burning velocity of $NH_3/H_2/Air$ flame with (a) different equivalence ratios and hydrogen fractions, (b) different inlet temperature and inlet pressure and (c) different oxygen contents in the oxidizer (Intersection point with laminar burning velocity of methane flame under NTP: •).
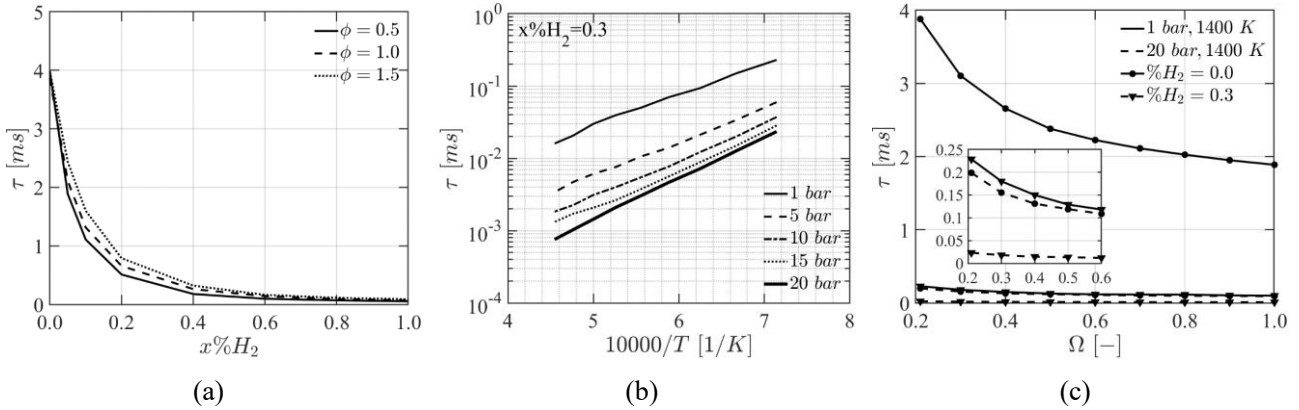
5.2 Ignition delay

As ammonia flame requires a high ignition energy, an improvement of ignition delay for ammonia flames and ammonia/hydrogen flames is necessary for ignition system design in the combustor of the LJEG. Figure 6(a) shows ignition delay time versus hydrogen blending ratio from 0.0 to 1.0 at different equivalence ratios at the inlet temperature of $1400\ K$ and inlet pressure of $1\ bar$. A small fraction $(0.0 - 0.2)$ of hydrogen addition may exponentially reduce ignition delay time and effectively enhance ignition robustness. With a further increase of hydrogen blending ratio, ignition delay shows relatively smaller improvement. Sensitivity analysis on OH radical at ignition moment has been conducted to identify the most important reactions in shortening ignition delay. Ten normalised sensitivity coefficients (the top 5 positive and the top 5 negative) are shown for each case in Figure 7. As shown in Figure 7(a) and (b), $O_2 + H = O + OH$ is the dominate reaction in both pure ammonia and $80\%NH_3/20\%H_2$ blends. When 20% hydrogen is introduced into the fuel blends, the second active reaction is changed from $NH_3 + NH_2 = N_2H_3 + H_2$ to $H_2 + OH = H + H_2O$ that consumes hydrogen and yields H radical to promote ignition of ammonia. Also, the inhibitive reactions $NH_3 + H = NH_2 + H_2$ and $NH_2 + NH_2 = N_2H_2 + H_2$ become less sensitive with $80\%NH_3/20\%H_2$ blends. This results in the promoting effect on ignition behaviour with hydrogen addition.

It is concluded from Figure 6(a) that equivalence ratio shows larger impact on ignition delay as hydrogen blending ratio is around 0.2. When hydrogen blending ratio is high, equivalence ratio plays a less important role to affect ignition delay. Figure 7(c) and (d) further demonstrate the normalized sensitivity coefficients of OH with the equivalence ratio of 0.5 and 1.5 when hydrogen blending ratio is 0.2. The most sensitive reactions are similar in both cases. Elementary reactions $O_2 + H = O + OH$ and $H_2 + OH = H + H_2O$ are dominant for the promoting effect, while $NH_3 + OH = NH_2 + H_2O$ and $NH_2 + NH_2 = N_2H_2 + H_2$ are the reactions responsible for ignition suppression. The chain branching reaction $O_2 + H = O + OH$ is promoted under fuel-lean conditions as more oxygen is involved in, which explains the shortened ignition delay time at $\phi = 0.5$ as shown in Figure 6(a).

Apart from hydrogen blending ratio and equivalence ratio, inlet temperature and inlet pressure have important effects on ignition delay. Figure 6(b) illustrates ignition delay with hydrogen blending ratio of 0.3 at the equivalence ratio of 1.1. It is found that ignition delay time is shortened as the inlet temperature and inlet pressure increases. However, the influences of pressure on ignition delay decreases as pressure rises. For the case of $70\%NH_3/30\%H_2$ flame, a factor $(\tau_{1bar}/\tau_{5bar})$ between $1\ bar$ and $5\ bar$ is around 4.7 with the inlet temperature at $1800\ K$ $(10000/T = 5.56)$, which is more than two times of the factor $(\tau_{5bar}/\tau_{10bar} \sim 1.9)$ between $5\ bar$ and $10\ bar$. It indicates that inlet pressure changes from $1 - 5\ bar$ has a great impact on reducing ignition delay, whilst moderate ignition delay improvement is achieved with further pressure increments.

Oxygen enrichment has its impact on ignition delay as well. As shown in Figure 6(c), the increase of oxygen content in oxidizer improves ignition of both ammonia and $70\%NH_3/30\%H_2$ flames. Ignition delay time is shortened as the oxidizer changes from air to pure oxygen under ambient pressure condition. Figure 7(e) and (f) illustrate the most significant promoting reactions are $O_2 + H = O + OH$ and $NH_3 + NH_2 = N_2H_3 + H_2$. Similar to the previous discuss, $NH_3 + H = NH_2 + H_2$ and $NH_2 + NH_2 = N_2H_2 + H_2$ have the significant retarding effect on ignition of ammonia combustion. With higher oxygen concentration in oxidizer, normalized sensitivity coefficients of the top five promoting reactions indicate more active reactions take place, e.g., the reaction $NH_3 + NH_2 = N_2H_3 + H_2$. As a result, ignition delay time is commonly reduced under oxygen-

enriched conditions. Nevertheless, under atmospheric pressure, ignition delay time decrease attributes more to hydrogen blending instead of oxygen enrichment. When 30% hydrogen is blending in the fuel at $1\ bar$, the ignition delay time is almost equivalent to that of pure ammonia at $20\ bar$. Under high pressure ($20\ bar$), for either pure ammonia or ammonia/hydrogen mixture, limited benefit would be brought by more oxygen involved in oxidizer. In the LJEG common work condition, the pressure in the external combustor will be maintained in the range of $10-20\ bar$, which indicates an increase of oxygen content in oxidizer having limited positive impact on solving ammonia ignition delay along with hydrogen addition as a combustion promoter.

(a)　　　　　　　　　　(b)　　　　　　　　　　(c)

Figure 6. Ignition delay time as a function of (a) various equivalence ratios and hydrogen blending ratios, (b) various inlet temperature and inlet pressure and (c) various oxygen contents in the oxidizer.

(a)　　　　　　　　　　　　　　　　(b)

(c)   (d)

(e)   (f)
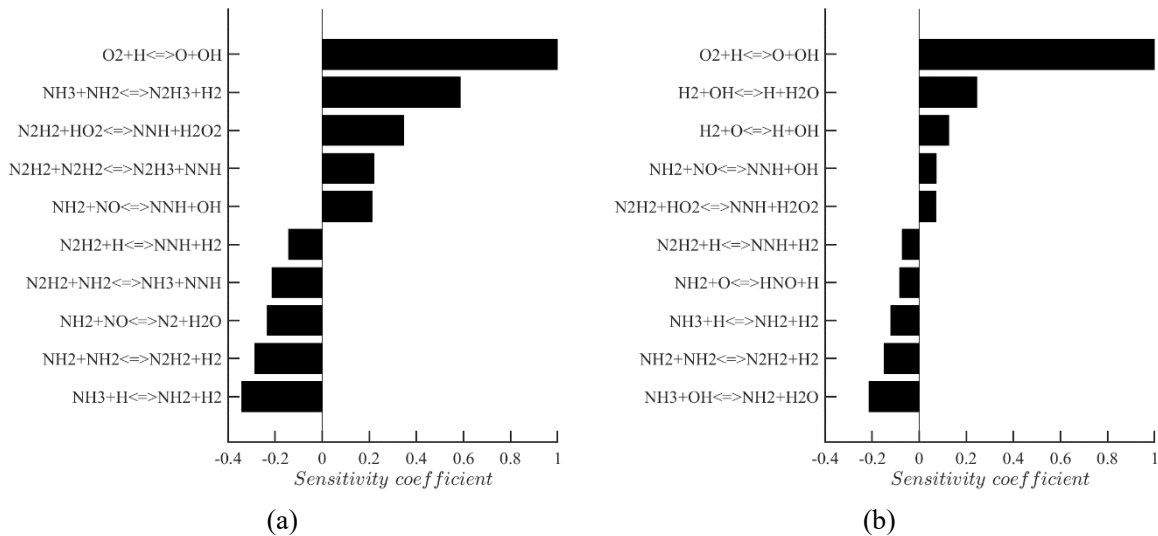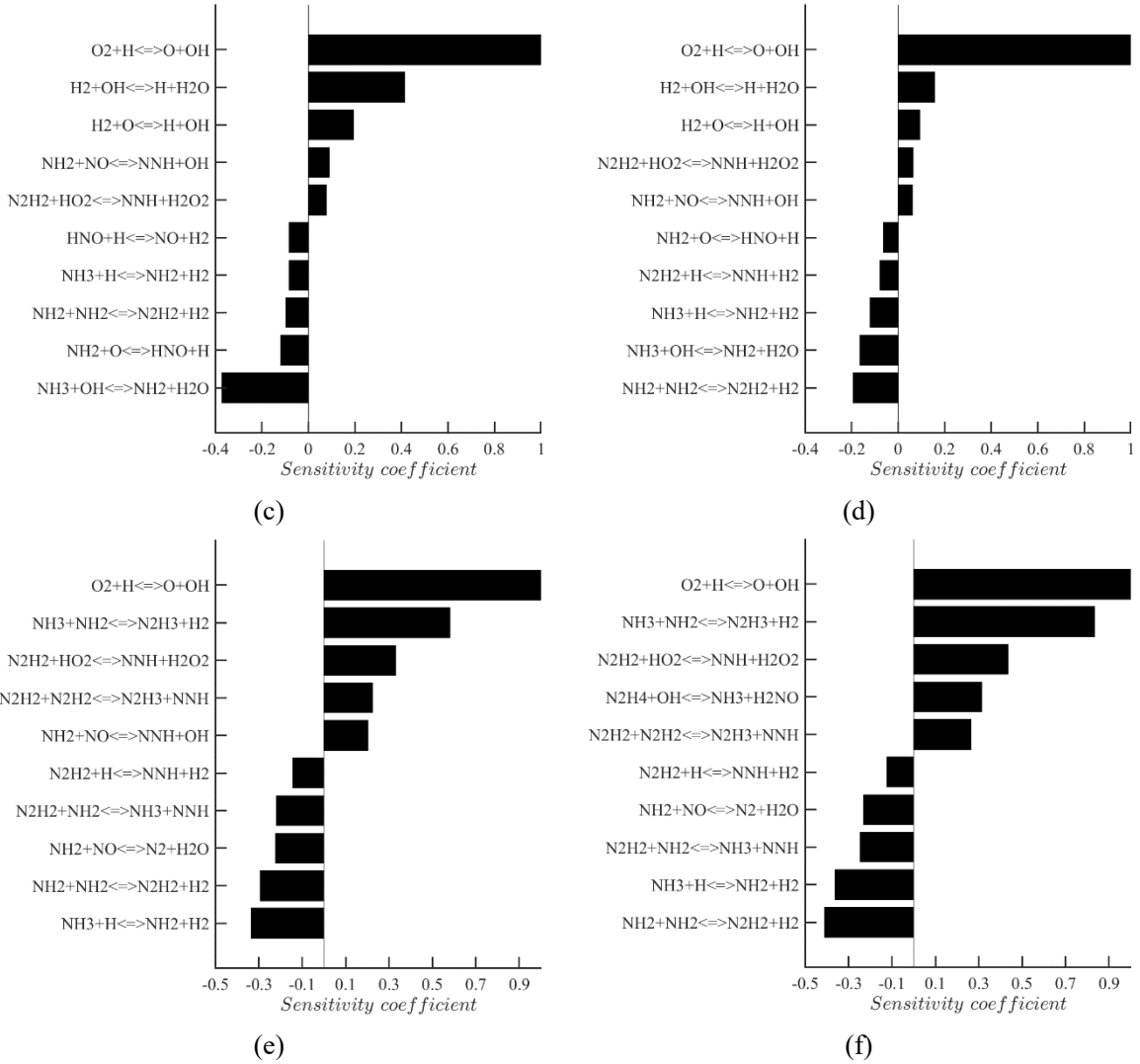
Figure 7. Normalized sensitivity analysis of OH with (a) $x\%H_2 = 0.0$, (b) $x\%H_2 = 0.2$, (c) $\phi = 0.5$, (d) $\phi = 1.5$, (e) $\Omega = 0.21$ and (f) $\Omega = 1.00$. (a-b): $\phi = 1, T = 1400\ K, P = 1\ bar, \Omega = 0.21$; (c-d): $x\%H_2 = 0.2, T = 1400\ K, P = 1\ bar, \Omega = 0.21$; (e-f): $\phi = 1.1, x\%H_2 = 0.0, T = 1400\ K, P = 1\ bar$.

5.3 Flame species

An important issue associating with any ammonia-combusted heat engines is NO_x emission. Ammonia has complex reaction routes in a nitrogen rich environment. It is interesting to understand how fuel-bound nitrogen of ammonia and hydrogen blending to impact NO_x formation under the working conditions of the LJEG. In this section, flame species mole fraction profiles under various conditions are generated from the model and rate of production (ROP) analysis is conducted to get insights of flame species concentrations.
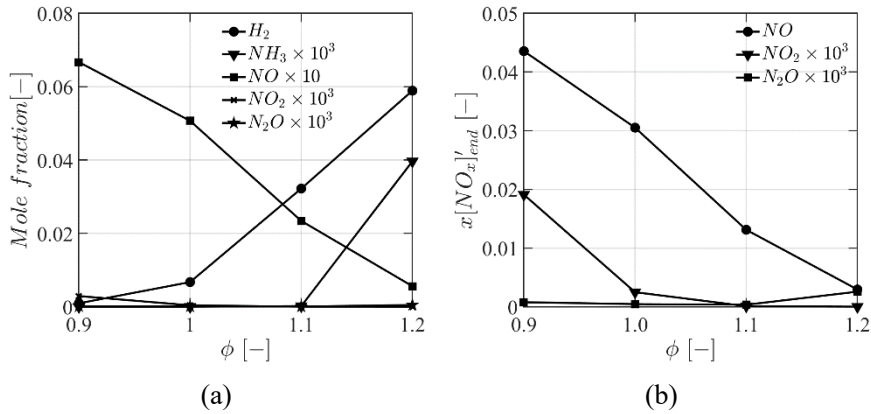
Figure 8(a) depicts the mole fractions of $NH_3, H_2, NO, NO_2, N_2O$ emissions at the equivalence ratio from $0.9 - 1.2$ for a $70\%NH_3/30\%H_2$ flame. The detailed inlet components are shown in Table 3. It can be seen that NO_2 and N_2O emissions are nearly zero and the dominant NO_x emission in ammonia/hydrogen combustion is NO, which shares the same trend in hydrocarbon premixed flames. As equivalence ratio increases, NO emission is decreased considerably, particularly when the equivalence ratio is slightly above unity. Additionally, it is noted in Figure 8(a) that hydrogen concentration is increased significantly with an equivalence ratio higher than unity. Unburnt ammonia is also increased when the equivalence ratio is higher than 1.1. To avoid abundant hydrogen and ammonia in rich flames and high NO_x emission in lean flames, an equivalence ratio of $1.0 < \phi < 1.1$ is

12

385   favourable for emission control, which also aligns with the recommendation from the previous analysis of

386   combustion robustness (Fig. 5(a), section 5.1). In Table 3, the mole fraction of inlet ammonia increases when

387   hydrogen blending ratio and oxygen content in the oxidizer keep constant. In order to avoid the effect of various

388   inlet ammonia amount on NO_x emission, normalized NO is calculated by dividing by the amount of inlet

389   ammonia. It is illustrated in Figure 8(b) that normalized NO is significantly decreased at the rich flames.

390

391   In Figure 9, the ROP analysis of NO with the equivalence ratios of 0.9 and 1.2 represents the cases of the lean

392   flame and the rich flame. In the lean flame, NO is mostly formed through fuel-bound NO ($HNO + H = NO +$

393   $H_2, HNO + OH = NO + H_2O$) and partly through thermal-NO, while NO is consumed primarily through the

394   reaction with NH_i (NH, NH_2) and partly through the reverse reaction of thermal-NO mechanism ($N_2 +$

395   $O = NO + N$). In the rich flame, the production from fuel-bound NO decreases while that from thermal-

396   NO increases, and the consumption is mainly through the reverse thermal-NO mechanism. The results align with

397   a recent study indicating that the contribution of NH_i oxidation via HNO for NO formation trends to be

398   restrained due to the decrease of $O/H/OH$ radicals in rich flames [53]. Besides, the reaction of NH_i and H is

399   promoted with the increase of H concentration in rich flame, resulting in high production of nitrogen atoms (N),

400   in turn, promoting the consumption of NO through the reversed thermal-NO mechanism. As a result, NO

401   concentration is reduced in rich flame, which helps to explain the NO profile in Figure 8(a).

402   Table 3 Inlet components under various equivalence ratio.

Case	ϕ	$x\%H_2$	Ω	$x[NH_3]$	$x[H_2]$	$x[O_2]$	$x[N_2]$
1	0.9			0.15	0.07	0.16	0.62
2	1.0	0.3	0.21	0.17	0.07	0.16	0.60
3	1.1			0.18	0.08	0.16	0.59
4	1.2			0.19	0.08	0.15	0.58

403

(a)   (b)

404   Figure 8. Mole fractions of $NH_3, H_2, NO, NO_2, N_2O$ emissions and normalized NO_x emission at various

405   equivalence ratio for a $70\%NH_3/30\%H_2$ flame ($T = 500\ K, P = 1\ bar$).
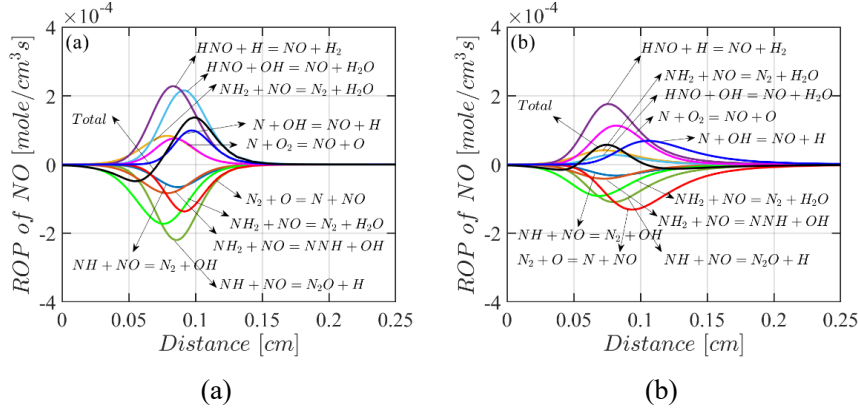
Figure 9. ROP analysis of NO at (a) $\phi = 0.9$ and (b) $\phi = 1.2$.

In Figure 10(a), the effect of hydrogen fraction in fuel blend on emissions of ammonia/hydrogen flame is discussed at the equivalence ratio of 1.1. Table 4 presents the inlet mole fractions of components varying with the hydrogen blending ratio. NO emission only increases marginally and unburnt hydrogen in the post-flame zone seems to be similar, although more hydrogen fraction in the fuel blend. In Figure 10(b), normalized NO concentration (against inlet ammonia mole fraction) increases apparently due to the decrease of inlet ammonia mole fraction shown in Table 4. Through the ROP analysis in Figure 11, it is concluded that although the production rates of both fuel-bound NO and thermal-NO rise under a higher hydrogen blending ratio, thermal-NO $(N_2 + O = N + NO)$ has a greater impact on NO consumption. Extra NO consumption may dynamically balance most of intensified NO production. Consequently, it shows a marginal increase of NO concentration in the post-flame zone. The similar hydrogen mole concentration in the post-flame zone exhaust with different hydrogen fraction in fuel mixture is explained using the hydrogen ROP analysis illustrated in Figure 12. Hydrogen is mainly formed through the reactions of NH_i $(NH_3, NH_2, NH, N_2H_2) + H$, the reaction of NH_i (e.g. $NH_2 + NH_3, NH_2 + NH_2$) as well as $HNO + H$. Hydrogen is mainly consumed through the hydrogen oxidation ($H_2 + O$ and $H_2 + OH$). As hydrogen mole fraction in the fuel rises, the hydrogen oxidation is promoted, especially, the reaction of $H_2 + OH = H + H_2O$. Hence, although more hydrogen is introduced into the fuel, the unburnt hydrogen in the post-flame zone at $\phi = 1.1$ keeps almost the same.

Table 4 Inlet components under various hydrogen blending ratio.

Case	ϕ	$x\%H_2$	Ω	$x[NH_3]$	$x[H_2]$	$x[O_2]$	$x[N_2]$
1		0.0		0.24	0.00	0.16	0.60
2		0.1		0.22	0.02	0.16	0.60
3	1.1	0.2	0.21	0.20	0.05	0.16	0.59
4		0.3		0.18	0.08	0.16	0.59
5		0.5		0.13	0.13	0.15	0.58
6		0.8		0.06	0.24	0.15	0.56

(a)   (b)
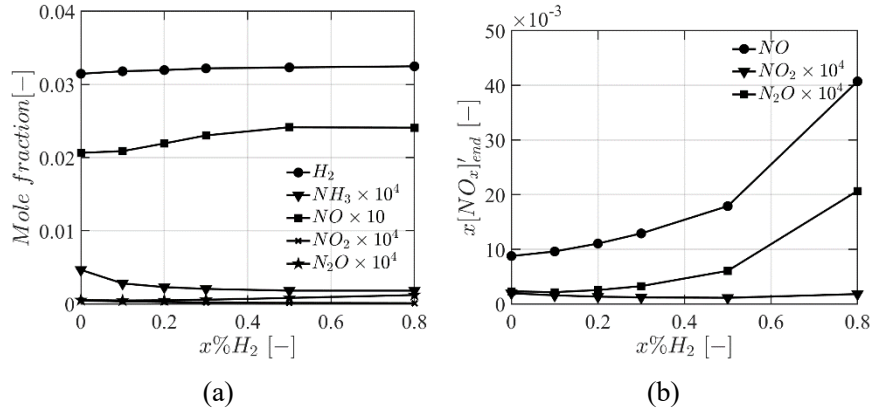
Figure 10. Mole fractions of $NH_3, H_2, NO, NO_2, N_2O$ emissions and normalized NO_x emission at different hydrogen blending ratios $(\phi = 1.1, T = 500\ K, P = 1\ bar)$.

(a)   (b)   (c)
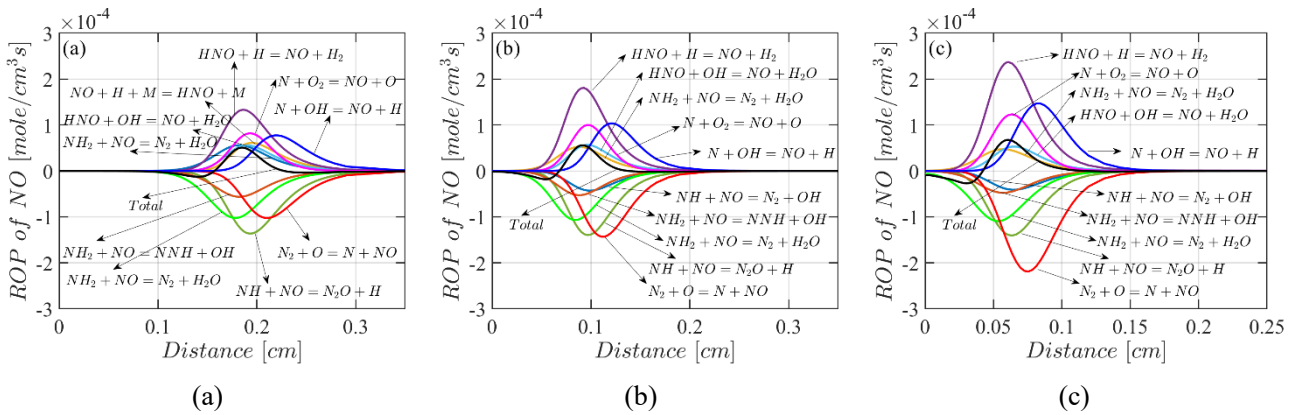
Figure 11. ROP analysis for NO at (a) $x\%H_2 = 0.0$, (b) $x\%H_2 = 0.2$ and (c) $x\%H_2 = 0.5$.

(a)   (b)   (c)

Figure 12. ROP analysis for H_2 at (a) $x\%H_2 = 0.0$, (b) $x\%H_2 = 0.2$ and (c) $x\%H_2 = 0.5$.
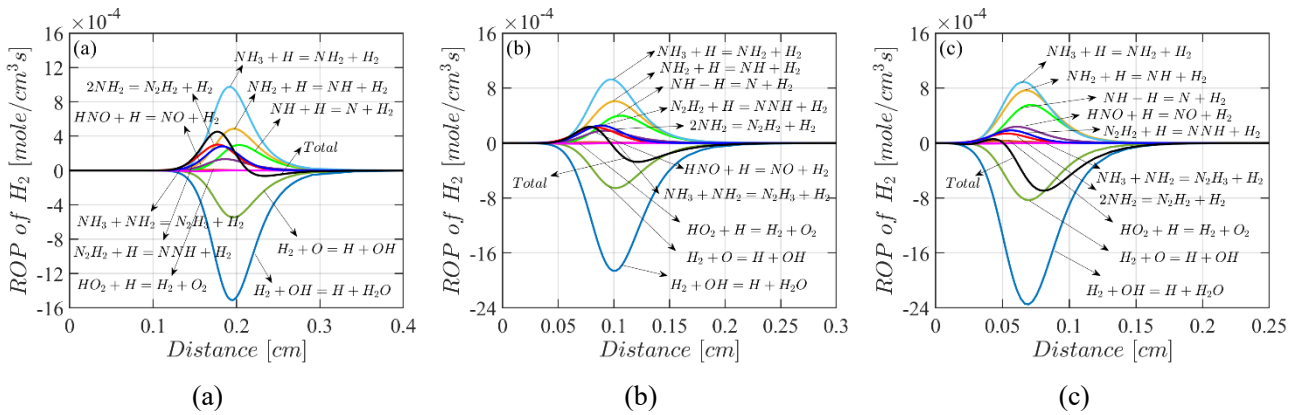
The effects of oxygen content in oxidizer are studied based on the case of $70\%NH_3/30\%H_2$ flames $(\phi = 1.1)$. The mole fractions of inlet components are demonstrated in Table 5. In Figure 13(a), it is noted that NO concentration in exhaust rises when more nitrogen in oxidizer is replaced by oxygen. From the perspective of ROP, it is revealed that the main paths of production and consumption remain the same even though the oxygen content in oxidizer increases from 0.21 (air) to 1.00 (pure oxygen) in Figure 14. Fuel-bound NO reaction $(HNO + H = NO + H_2)$ is dominant in NO production and thermal NO reaction $(N_2 + O = N + NO)$ is dominant in consumption, although the rates of both production and consumption are promoted almost twice while pure oxygen is used as the oxidizer. As the equivalence ratio and the hydrogen blending ratio keep constant

15

437   (see Table 5), the ammonia concentration is increased in the fuel when the oxygen content is enhanced in oxidizer.

438   Thus, the normalized NO emission is decreased as shown in Figure 13(b). It is concluded that the increase of

439   absolute NO emission is caused by the result of offsetting in NO production and consumption, but normalised

440   NO emission reduction is because the ammonia concentration involved in the fuel blend as the denominator

441   increases with the increase of oxygen concentration to keep a constant equivalence ratio. With more oxygen

442   content is introduced in the oxidizer, absolute NO_2 and N_2O emissions are also enhanced. In Figure 13(b), the

443   normalised NO_2 and N_2O emissions minimise the impact of higher fractions of ammonia, which shows limited

444   benefits would be brought with pure oxygen as the oxidizer for normalised NO_2 emission, while normalised

445   N_2O emission has a decreasing trend.

446

Table 5 Inlet components under various oxygen contents in the oxidizer.

Case	ϕ	$x\%H_2$	Ω	$x[NH_3]$	$x[H_2]$	$x[O_2]$	$x[N_2]$
1			0.21	0.18	0.08	0.16	0.59
2			0.4	0.28	0.12	0.24	0.36
3	1.1	0.3	0.6	0.35	0.15	0.30	0.20
4			0.8	0.40	0.17	0.35	0.09
5			1	0.43	0.19	0.38	0.00

447

(a)   (b)
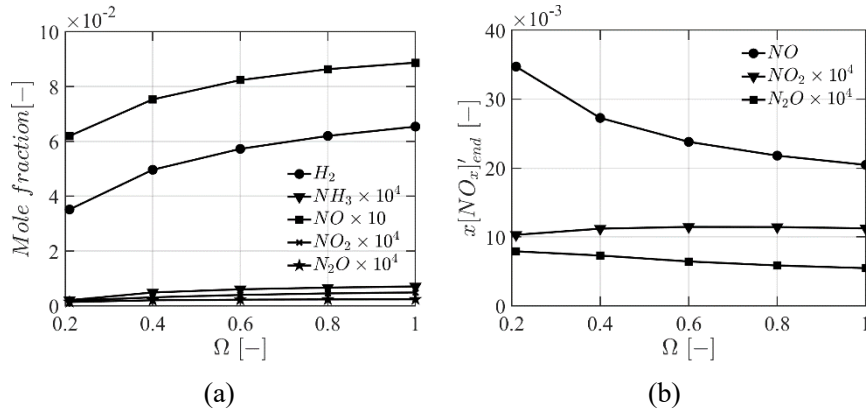
448   Figure 13. Mole fractions of $NH_3, H_2, NO, NO_2, N_2O$ emissions and normalized NO_x emission with oxygen

449   content at the range of $0.21 - 1.00$ for $70\%NH_3/30\%H_2$ flame ($\phi = 1.1, T = 500\ K, P = 1\ bar$).

(a)   (b)
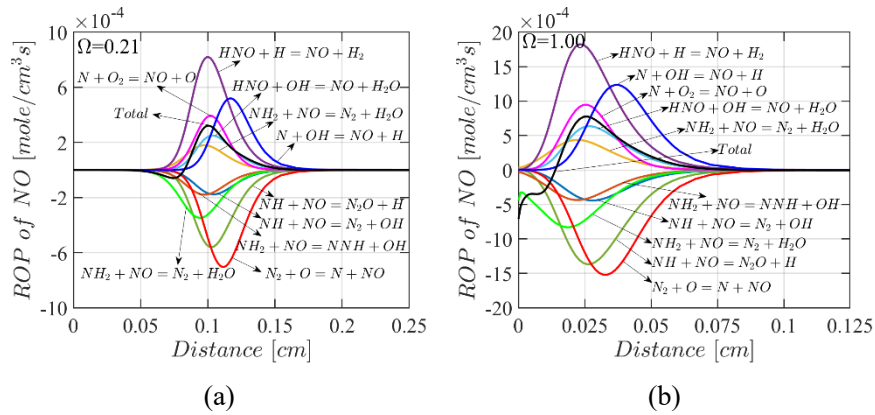
450   Figure 14. ROP analysis for NO with (a) 0.21 and (b) 1.00 oxygen content in the oxidizer at $T =$

451    $500\ K, P = 1\ bar$.

452   To involve in the consideration of high-pressure work conditions in the LJEG, a comparison is conducted based

453   on different inlet pressures $(1 - 20 \ bar)$. In Figure 15, emissions are illustrated under various inlet pressures
454   (the same inlet temperature of $600 \ K$ and an equivalence ratio of 1.1). There is a clear trend of NO emission
455   decreasing as inlet pressure rises. The change is more significant from $1 \ bar$ to $10 \ bar$ compared to that from
456    $10 \ bar$ to $20 \ bar$. A similar finding is mentioned in the study of premixed ammonia/methane combustion [17].
457   An explanation was raised in [53] that the combination of NH_i radical is promoted under high pressure (or fuel-
458   rich conditions), which promotes to yield nitrogen instead of NO. This finding suggests that typical high-pressure
459   in the external combustor of the LJEG is a favourable environment for NO reduction when a $70\%NH_3/30\%H_2$
460   fuel blend is utilized.
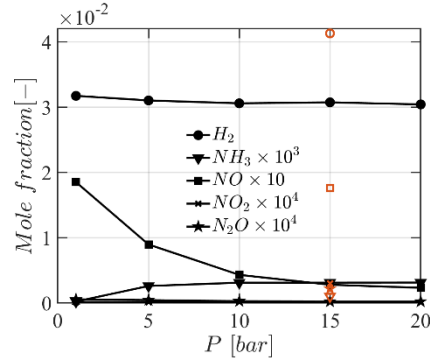
461
462   Figure 15. Emissions of $NH_3, H_2, NO, NO_2, N_2O$ under different inlet pressure for $70\%NH_3/30\%H_2$
463   flame $(\phi = 1.1, \Omega = 0.21, T = 600 \ K)$; The red points illustrate the emission species at the optimized inlet
464   parameters of LJEG, i.e. $\phi = 1.1, x\%H_2 = 0.3, \Omega = 0.3, T = 600 \ K, P = 15 \ bar$.

465   **5.4   Selected operational parameters for the external combustor of the LJEG**
466   Following the comprehensive investigation of the impacts of various operational parameters on ammonia
467   combustion and emissions, a general recommendation to realize stable, efficient and environment friendly
468   operation of the ammonia fuelled LJEG is given with the clear aim to enhance ammonia combustion robustness
469   and minimise NO_x emission.

470

471   The laminar burning velocity of methane flames $(\sim 37 \ cm/s)$ sets a benchmark for ammonia flames enhanced
472   with combustion promoter and favourable operational parameters. Hydrogen, as a combustion promoter with its
473   high burning velocity, could easily improve the burning velocity of premixed ammonia/hydrogen flame to exceed
474    $37 \ cm/s$. However, a high fraction of hydrogen in ammonia/hydrogen blends requires highly efficient premium
475   catalysts to crack ammonia online or a separate hydrogen fuel supply line. To achieve a cost-effective solution to
476   promote ammonia combustion robustness, hydrogen addition has to be considered along with other operational
477   parameters, e.g. equivalence ratio, pressure and temperature. Equivalence ratio between 1.1 and 1.2 is
478   beneficial to reach a higher burning velocity in most cases. In regard to inlet pressure and temperature of the
479   ammonia combustor, they are not fully independent parameters which are largely determined by thermodynamic
480   parameters at the compressor outlet of the LJEG. Inlet temperature has a monotonical positive impact on burning
481   velocity while high inlet pressure prohibits burning velocity increase. At a typical outlet condition of $600 \ K$ and
482    $15 \ bar$, a $70\%NH_3/30\%H_2$ fuel blend $(\phi = 1.1)$ achieves the laminar burning velocity slightly above
483    $40 \ cm/s$ (see Figure 5(b)). This satisfies the requirement of the ammonia combustor regarding combustion
484   robustness when a stable flame is formed. Oxygen enrichment also has a significant and positive impact on
485   burning velocity, which may need a detailed economic analysis to reach a more economically viable solution.
486   Further considerations also need to be put on ignition delay and NO_x emission to determine an all-rounder
487   solution.

488

489   In terms of ignition delay, as discussed in Section 5.2, 20% hydrogen addition already significantly reduces

490   ignition delay time nonetheless 30% hydrogen addition applied. The common work condition of the LJEG, i.e.,

491   15 bar at the inlet of the external combustor, has a major effect on reducing ignition delay. Jointly, the

492   requirement of a short ignition delay also can be met with the abovementioned condition, i.e., 30% hydrogen

493   addition, 15 bar inlet pressure and equivalent ratio of 1.1.

494

495   As discussed in Section 5.3, different operational parameters have complicated synergies on flame species,

496   especially, NO_x emission of the greatest interest. Equivalence ratio between 1.0 and 1.1 is widely accepted in

497   almost all literatures studying ammonia combustion. In rich burn, NO_x emission can be suppressed even lower,

498   however increasing amount of hydrogen in exhaust is equally unacceptable in the LJEG, where after-burn device

499   may be required which would further increase overall NO_x emission. In practical situations, rich burn with a

500   high equivalence ratio may lead to ammonia slip if the external combustor of the LJEG was not optimally designed.

501   Therefore, a moderate equivalence ratio of 1.1 as selected for combustion robustness is equally acceptable here.

502   In terms of hydrogen addition, the selected fraction (30%) is ideal as a further increase of hydrogen fraction

503   leads to intensified thermal-NO production which eventually pushes up NO emission as seen in Figure 10(a).

504   Besides hydrogen addition and equivalence ratio, the most important operational parameters to affect NO_x

505   emission are oxygen content in oxidizer and inlet pressure of the combustor. NO_x emission decrease

506   monotonically while higher oxygen concentration and higher pressure are applied. Although absolute mole

507   fractions of NO_x upsurge when higher absolute oxygen concentrations are applied, the normalised NO and

508   N_2O emissions demonstrate a decreasing trend in Figure 13(b). A moderate oxygen concentration of 30% is

509   selected subject to a further investigation on economic viability of its application on the LJEG.

510

511   With the advantageous parameter combination of equivalence ratio, hydrogen addition, and oxygen content, and

512   the typical input parameters of the LJEG ($T = 600\ K, P = 15\ bar$), the concentration of NH_3, H_2, NO_x

513   species are marked in Figure 15. Mole fractions of unburnt H_2 and NO emissions are around 4.1% and 1.7%,

514   respectively, while those of NO_2, N_2O and unburnt NH_3 are negligible. Moreover, both the formation and

515   consumption of NO is dominated by fuel-bound NO reactions (reaction with HNO or NH). It is anticipated

516   that the selected operational parameters offer a great guidance on the design of the ammonia combustor with

517   elevated inlet pressure in the LJEG. The general conclusion of the impacts of operational parameters on ammonia

518   combustion robustness and emissions provides a useful reference for other combustion device developments.

519

520 **6. Conclusions**

521   The combustion characteristics of premixed ammonia/hydrogen are investigated by applying detailed chemical

522   kinetic modelling to support the combustion system development of an ammonia/hydrogen dual-fuelled Linear

523   Joule Engine Generator (LJEG). An ammonia combustion mechanism is selected from several representative

524   mechanisms based on the validation against the same set of experimental data. Laminar burning velocity, ignition

525   delay and flame species concentration are investigated over a wide range of equivalence ratios, hydrogen blending

526   ratios, oxygen content in the oxidizer, inlet temperature and pressure, which are related to typical LJEG operating

527   conditions. Rate of production (ROP) analysis is utilized to gain a deeper insight into the NO_x formation and

528   consumption pathways. The findings obtained from this study indicate the potential of realizing robust and low

529   NOx emission combustion in the proposed LJEG prototype. The major conclusions are summarised as follows.

530   ●   With the increase of equivalence ratio, NO concentration decreases and concentrations of unburnt H_2 and

531   NH_3 increases notably, while laminar burning velocity peaks at around 1.1. This suggests that an

532   equivalence ratio of 1.1 is beneficial for both combustion robustness and emission reduction.

- Both adding hydrogen in the fuel and enriching oxygen in the oxidizer effectively promote the laminar burning velocity and reduce the ignition delay of ammonia. 40% hydrogen in fuel or 60% oxygen in oxidizer can increase the burning velocity of ammonia to the similar level of methane (37 cm/s under ambient temperature and pressure condition). Adding hydrogen results in marginal increase in NO emission. Apparent increase of absolute NO emission is found in the oxygen-enriched environment, but normalised NO and N_2O emissions demonstrate decreasing trends.
- Increase of inlet pressure tends to suppress burning velocity, however, the effects reduce as the pressure is further elevated. Ignition delay is shortened as pressure increases; however, the effects diminish at a higher pressure. NO emission falls significantly with the elevation of pressure.
- Considering the impacts of different parameters, a favorable combination, i.e., $30\%H_2/70\%NH_3, \Omega = 0.3$, $\phi = 1.1$, $T_1 = 600\ K, P_1 = 15\ bar$ is selected. Result shows NO emission is around 1.7% while those of NO_2 and N_2O are negligible, offering a great guidance on the design of the ammonia combustor to minimize emissions.
- ROP analysis indicates that both fuel-bound NO reactions and thermal NO reactions play important role in NO production and consumption. The relative importance of those two pathways and the individual reactions within each pathway vary with the parameters studied, and lead to the phenomena observed in the parametric study.

Conflicts of Interest: The authors declare no conflict of interest.

References

[1] Zamfirescu C, Dincer I. Using ammonia as a sustainable fuel. Journal of Power Sources. 2008;185:459-65.

[2] Valera-Medina A, Xiao H, Owen-Jones M, David WIF, Bowen PJ. Ammonia for power. Progress in Energy and Combustion Science. 2018;69:63-102.

[3] Morgan E, Manwell J, McGowan J. Wind-powered ammonia fuel production for remote islands: A case study. Renewable Energy. 2014;72:51-61.

[4] Bicer Y, Dincer I, Zamfirescu C, Vezina G, Raso F. Comparative life cycle assessment of various ammonia production methods. Journal of Cleaner Production. 2016;135:1379-95.

[5] Brohi EA. Ammonia as fuel for internal combustion engines? An evaluation of the feasibility of using nitrogen-based fuels in ICE. Gothenburg, Sweden: Chalmers University of Technology; 2014.

[6] Gray JT, Dimitroff E, Meckel NT, Quillian RD. Ammonia Fuel – Engine Compatibility and Combustion. SAE International; 1966.

[7] Pratt DT. Performance of Ammonia-Fired GasTurbine Combustors: Berkley University of California; 1967.

[8] Kurata O, Iki N, Matsunuma T, Inoue T, Tsujimura T, Furutani H, et al. Performances and emission characteristics of NH3 – air and NH3CH4 – air combustion gas-turbine power generations. Proceedings of the Combustion Institute. 2017;36:3351-9.

[9] SIP energy carriers 2016. Japan Science and Technology Agency; 2016.

[10] Wu D, Roskilly AP. Design and Parametric Analysis of Linear Joule-cycle Engine with Out-of-

577   cylinder Combustion. Energy Procedia. 2014;61:1111-4.

578   [11] Ngwaka U, Wu D, Happian-Smith J, Jia B, Smallbone A, Diyoke C, et al. Parametric analysis of

579   a semi-closed-loop linear joule engine generator using argon and oxy-hydrogen combustion. Energy.

580   2020.

581   [12] Generation P. Reliable gas turbines.

582   [13] Jia B, Wu D, Smallbone A, Lawrence C, Roskilly AP. Design, modelling and validation of a

583   linear Joule Engine generator designed for renewable energy sources. Energy Conversion and

584   Management. 2018;165:25-34.

585   [14] Ngwaka U, Jia B, Lawrence C, Wu D, Smallbone A, Roskilly AP. The characteristics of a Linear

586   Joule Engine Generator operating on a dry friction principle. Applied Energy. 2019;237:49-59.

587   [15] Grannell SM, Assanis DN, Bohac SV, Gillespie DE. The Fuel Mix Limits and Efficiency of a

588   Stoichiometric, Ammonia, and Gasoline Dual Fueled Spark Ignition Engine. Journal of Engineering

589   for Gas Turbines and Power. 2008;130.

590   [16] Okafor EC, Naito Y, Colson S, Ichikawa A, Kudo T, Hayakawa A, et al. Experimental and numerical

591   study of the laminar burning velocity of CH_4–NH_3–air premixed flames. Combustion and Flame.

592   2018;187:185-98.

593   [17] Xiao H, Valera-Medina A, Bowen PJ. Study on premixed combustion characteristics of co-firing

594   ammonia/methane fuels. Energy. 2017;140:125-35.

595   [18] Ichikawa A, Naito Y, Hayakawa A, Kudo T, Kobayashi H. Burning velocity and flame structure of

596   CH_4/NH_3/air turbulent premixed flames at high pressure. International Journal of Hydrogen Energy.

597   2019;44:6991-9.

598   [19] Lee JH, Kim JH, Park JH, Kwon OC. Studies on properties of laminar premixed hydrogen-added

599   ammonia/air flames for hydrogen production. International Journal of Hydrogen Energy. 2010;35:1054-

600   64.

601   [20] Valera-Medina A, Pugh DG, Marsh P, Bulat G, Bowen P. Preliminary study on lean premixed

602   combustion of ammonia-hydrogen for swirling gas turbine combustors. International Journal of

603   Hydrogen Energy. 2017;42:24495-503.

604   [21] Joo JM, Lee S, Kwon OC. Effects of ammonia substitution on combustion stability limits and

605   NOx emissions of premixed hydrogen–air flames. International Journal of Hydrogen Energy.

606   2012;37:6933-41.

607   [22] Khateeb AA, Guiberti TF, Wang G, Boyette WR, Younes M, Jamal A, et al. Stability limits and

608   NO emissions of premixed swirl ammonia-air flames enriched with hydrogen or methane at elevated

609   pressures. International Journal of Hydrogen Energy. 2021;46:11969-81.

610   [23] Mathieu O, Petersen EL. Experimental and modeling study on the high-temperature oxidation of

611   Ammonia and related NOx chemistry. Combustion and Flame. 2015;162:554-70.

612   [24] Konnov AA. Implementation of the NCN pathway of prompt-NO formation in the detailed reaction

613   mechanism. Combustion and Flame. 2009;156:2093-105.

614   [25] Li J, Huang H, Kobayashi N, He Z, Osaka Y, Zeng T. Numerical study on effect of oxygen content

615   in combustion air on ammonia combustion. Energy. 2015;93:2053-68.

616   [26] Takeishi H, Hayashi J, Kono S, Arita W, Iino K, Akamatsu F. Characteristics of ammonia/N2/02

617   laminar flame in oxygen-enriched air condition. Transactions of the JSME (in Japanese). 2015;81:14-

618   00423-14-.

619   [27] Mei B, Zhang X, Ma S, Cui M, Guo H, Cao Z, et al. Experimental and kinetic modeling investigation

620   on the laminar flame propagation of ammonia under oxygen enrichment and elevated pressure conditions.

621   Combustion and Flame. 2019;210:236-46.

622   [28] Wu F-H, Chen G-B. Numerical study of hydrogen peroxide enhancement of ammonia premixed flames.
623   Energy. 2020:118118.

624   [29] Barbas M, Costa M, Vranckx S, Fernandes RX. Experimental and chemical kinetic study of CO and
625   NO formation in oxy-methane premixed laminar flames doped with NH3. Combustion and Flame.
626   2015;162:1294-303.

627   [30] Mendiara T, Glarborg P. Ammonia chemistry in oxy-fuel combustion of methane. Combustion and
628   Flame. 2009;156:1937-49.

629   [31] Li Z, Li S. Kinetics modeling of NOx emissions characteristics of a NH3/H2 fueled gas turbine
630   combustor. International Journal of Hydrogen Energy. 2021;46:4526-37.

631   [32] Miller JA, Bowman CT. Mechanism and modeling of nitrogen chemistry in combustion. Progress in
632   Energy and Combustion Science. 1989;15:287-338.

633   [33] Li R, Konnov AA, He G, Qin F, Zhang D. Chemical mechanism development and reduction for
634   combustion of NH3/H2/CH4 mixtures. Fuel. 2019;257.

635   [34] Duynslaegher C, Contino F, Vandooren J, Jeanmart H. Modeling of ammonia combustion at low
636   pressure. Combustion and Flame. 2012;159:2799-805.

637   [35] Duynslaegher C, Jeanmart H, Vandooren J. Flame structure studies of premixed
638   ammonia/hydrogen/oxygen/argon flames: Experimental and numerical investigation. Proceedings of the
639   Combustion Institute. 2009;32:1277-84.

640   [36] Gregory PS, David MG, Michael F, Nigel WM, Boris E, Mikhail G, et al. GRI-Mech 3.0. 1999.

641   [37] Mechanical and Aerospace Engineering (Combustion Research) UoCaSD. Chemical-Kinetic Mechanisms
642   for Combustion Applications. 2005.

643   [38] Lindstedt RP, Lockwood FC, Selim MA. Detailed Kinetic Modelling of Chemistry and Temperature
644   Effects on Ammonia Oxidation. Combustion Science and Technology. 1994;99:253-76.

645   [39] Jiang B. Mécanisme de formation et de disparition des oxydes d'azote dans les flammes : étude
646   expérimentale et modélisation. Belgium: Université Catholique de Louvain; 1990.

647   [40] Meyer T, Kumar P, Li M, Redfern K, Diaz D. Ammonia combustion with near-zero pollutant
648   emissions. NH3 Congress. Iowa, USA2011.

649   [41] Song Y, Hashemi H, Christensen JM, Zou C, Marshall P, Glarborg P. Ammonia oxidation at high
650   pressure and intermediate temperatures. Fuel. 2016;181:358-65.

651   [42] Otomo J, Koshi M, Mitsumori T, Iwasaki H, Yamada K. Chemical kinetic modeling of ammonia
652   oxidation with improved reaction mechanism for ammonia/air and ammonia/hydrogen/air combustion.
653   International Journal of Hydrogen Energy. 2018;43:3004-14.

654   [43] Nakamura H, Hasegawa S, Tezuka T. Kinetic modeling of ammonia/air weak flames in a micro flow
655   reactor with a controlled temperature profile. Combustion and Flame. 2017;185:16-27.

656   [44] Bugler J, Somers KP, Simmie JM, Güthe F, Curran HJ. Modeling Nitrogen Species as Pollutants:
657   Thermochemical Influences. The Journal of Physical Chemistry A. 2016;120:7192-7.

658   [45] Dai L, Gersen S, Glarborg P, Levinsky H, Mokhov A. Experimental and numerical analysis of the
659   autoignition behavior of NH3 and NH3/H2 mixtures at high pressure. Combustion and Flame.
660   2020;215:134-44.

661   [46] Duynslaegher C. Experimental and numerical study of ammonia combustion. Belgium: Université
662   catholique de Louvain; 2011.

663   [47] Kumar P, Meyer TR. Experimental and modeling study of chemical-kinetics mechanisms for H2–
664   NH3–air mixtures in laminar premixed jet flames. Fuel. 2013;108:166-76.

665 [48] Lee JH, Lee SI, Kwon OC. Effects of ammonia substitution on hydrogen/air flame propagation
666 and emissions. International Journal of Hydrogen Energy. 2010;35:11332-41.
667 [49] Kwon OC, Faeth GM. Flame/stretch interactions of premixed hydrogen-fueled flames: measurements
668 and predictions. Combustion and Flame. 2001;124:590-610.
669 [50] Ichikawa A, Hayakawa A, Kitagawa Y, Kunkuma Amila Somarathne KD, Kudo T, Kobayashi H. Laminar
670 burning velocity and Markstein length of ammonia/hydrogen/air premixed flames at elevated pressures.
671 International Journal of Hydrogen Energy. 2015;40:9570-8.
672 [51] Wu K-K, Chang Y-C, Chen C-H, Chen Y-D. High-efficiency combustion of natural gas with 21–30%
673 oxygen-enriched air. Fuel. 2010;89:2455-62.
674 [52] Zhang W, Chen Z, Shen Y, Shu G, Chen G, Xu B, et al. Influence of water emulsified diesel &
675 oxygen-enriched air on diesel engine NO-smoke emissions and combustion characteristics. Energy.
676 2013;55:369-77.
677 [53] Kobayashi H, Hayakawa A, Somarathne KDKunkuma A, Okafor Ekenechukwu C. Science and technology
678 of ammonia combustion. Proceedings of the Combustion Institute. 2019;37:109-33.
679